



Published in final edited form as:

Org Biomol Chem. 2015 February 28; 13(8): 2474–2479. doi:10.1039/c4ob02433h.

Regulating Exocytosis of Nanoparticles via Host-Guest Chemistry

Chaekyu Kim[#], Gulen Yesilbag Tonga[#], Bo Yan, Chang Soo Kim, Sung Tae Kim, Myoung-Hwan Park, Zhengjiang Zhu, Bradley Duncan, Brian Creran, and Vincent M. Rotello^{*}

Department of Chemistry, University of Massachusetts, 710 North Pleasant Street, Amherst, MA 01003, USA

[#] These authors contributed equally to this work.

Abstract

Prolonged retention of internalized nanoparticulate systems inside cells improves their efficacy in imaging, drug delivery, and theranostic applications. Especially, regulating exocytosis of the nanoparticles is a key factor in the fabrication of effective nanocarriers for chemotherapeutic treatments but orthogonal control of exocytosis in the cellular environment is a major challenge. Herein, we present the first example of regulating exocytosis of gold nanoparticles (AuNPs), a model drug carrier, by using a simple host-guest supramolecular system. AuNPs featuring quaternary amine head groups were internalized into the cells through endocytosis. Subsequent *in situ* treatment of a complementary cucurbit[7]uril (CB[7]) to the amine head groups resulted in the AuNP-CB[7] complexation inside cells, rendering particle assembly. This complexation induced larger particle assemblies that remained sequestered in the endosomes, inhibiting exocytosis of the particles without any observed cytotoxicity.

Introduction

Drug delivery systems (DDSs) improve the efficacy of conventional pharmaceuticals through enhanced pharmacokinetics and biodistribution.¹ Finely tuned and engineered nanoparticle platforms² are used to design DDSs to achieve the release of drugs at a controlled rate.³ Trigger sensitive release mechanisms of covalently⁴ or non-covalently⁵ attached drugs are widely employed for on-target site activation strategies.⁶ Furthermore, much effort has focused on increasing the uptake of the carrier into targeted tissues passively through the enhanced permeability and retention (EPR) effect⁷ and/or actively by using targeting modalities.⁸ However, for effective DDSs, the sustained therapeutic effect inside cells relies not only on the cellular uptake of nanocarriers but also on their subsequent long-term retention in the cells.^{5c, 9}

One of the main obstacles of DDSs is the rapid removal of the internalized drug carriers through the exocytosis before the drug release.¹⁰ Exocytosis is the process of expelling

^{*} rotello@chem.umass.edu.

Electronic Supplementary Information (ESI) available: Synthesis of ligands, nanoparticles and characterization. See DOI: 10.1039/b000000x/

wastes and other large molecules out of the cells,¹¹ which is also commonly observed with a wide variety of drug carriers.¹² As an example, internalized poly (D,L-lactide-co-glycolide) nanoparticles undergo exocytosis to the extent of 65 % at 30 min and 85 % at 6 h.¹³ Reducing exocytosis of the nanoparticulate drug carriers thus prolong their retention time and concurrently release the loaded drugs gradually inside cells, enhancing the therapeutic efficiency of the DDSs.¹⁴ Developing strategies for orthogonal control of exocytosis in the cellular environment is a major challenge because of the intracellular chemical complexity and a potential toxicity of relevant reagents.

Supramolecular chemistry generates controlled assemblies from molecular building blocks through non-covalent interactions including hydrogen bonding, hydrophobic, and van der Waals interactions.¹⁵ Due to their reversible modularity, supramolecular complexes are useful for creating responsive host-guest systems for many therapeutic applications.¹⁶ Cucurbit[n]urils (CB[n]) are water-soluble macrocyclic hosts with a hydrophobic cavity that form strong inclusion complexes with many types of guests, including positively charged ligands on the gold nanoparticle (AuNP) surface.¹⁷ Various CB[n]-guest systems have been developed to create delivery vectors for therapeutic materials including drugs and an actuator system to control catalytic activity of an enzyme.¹⁸ Moreover, engineering host-guest systems provide the capability of actuation for the regulation of therapeutics in living cells.^{19,20} Among the cucurbituril family, cucurbit[7]uril (CB[7]) is attractive as a building block for the construction of supramolecular architectures due to its remarkable guest binding behavior in aqueous media²¹ and non-toxic behavior *in vitro* and *in vivo*.²²

Herein, we describe a new approach to regulate the exocytosis of AuNPs by using host-guest interactions between AuNPs and CB[7] molecules.²³ Quaternary ammonium functionalized cationic gold nanoparticles (AuNP-TBen) were readily taken up by the cells via endocytosis as reported in previous studies (Fig. 1).^{18c,24} Afterward, *in situ* treatment of complementary CB[7] molecules resulted in threading of CB[7]s on the terminal functionalities of AuNP-TBen inside the cells, resulting in AuNP-TBen-CB[7] complexes. This complexation rendered the surface of the particles less hydrophilic, inducing the self-assembly of AuNP-TBen-CB[7] sequestered in the endosomes. Exocytosis of the AuNP-TBen-CB[7] was then blocked by the increased size of the induced assemblies. This approach provides a new strategy for improving efficacy of drug delivery systems through prolonged retention of drug carriers within the cells.

Results and discussion

Exocytosis of nanoparticles is dependent on their size⁹ and surface functionality.²⁵ Compared to their smaller counterparts, larger nanoparticles (more than 100 nm in diameter) tend to undergo exocytosis at slower rate and lower amount. Therefore, an efficient way of regulating exocytosis could be inducing *in situ* assembly of internalized individual nanoparticles entrapped in endocytic vesicles by using a host-guest supramolecular system. The exocytosis of the particles then would be blocked by the increased size of the induced assemblies²⁶ and the host-guest system provides an orthogonal stimulus, allowing temporal control of the exocytosis (Fig. 1).

We have synthesized a water-soluble AuNP-TBen featuring a tetra(ethylene glycol) and quaternary benzyl amine head group prepared via a Murray place-exchange reaction.²⁷ The detailed syntheses and characterization of the AuNPs are available in the Supporting Information (Supporting Scheme 1 and Fig. 1-4). The gold core had an average size of 2.1 ± 0.5 nm with hydrodynamic diameter of the AuNP-TBen being 9.7 ± 0.1 nm determined by transmission electron microscope (TEM) and dynamic light scattering (DLS), respectively. The AuNP-TBen had a zeta potential of + 14.2 mV. The terminal quaternary benzyl amine moiety serves as a recognition unit for the formation of a host-guest inclusion complex with CB[7] with the association constant of $\sim 10^8 \text{ M}^{-1}$.²⁸ This higher binding constant is strong enough for the complexes to remain stable under biological conditions.²⁹

The complexation between AuNP-TBen and CB[7] was investigated by performing DLS experiments whose results are shown in Fig. 2(a). For DLS experiments, AuNPs were used at a concentration of 1 μM . At the molar ratio of 1:1 and 1:2 (AuNP-TBen:CB[7]), the hydrodynamic diameter of the AuNP-TBen slightly increased from 9.7 ± 0.1 to 11.6 ± 0.5 nm. At a ratio of 1:4 (AuNP-TBen:CB[7]), the particles began to assemble together and completely aggregated at the ratio of 1:10 (AuNP-TBen:CB[7]) to give a clear solution with a precipitation on the bottom of vial as shown in Fig. 1 (b). The hydrodynamic sizes of control nanoparticles including AuNP-TTMA and AuNP-TCOOH showed no observable change upon addition of CB[7] because both particles have no significant binding affinities to CB[7].

The formation of the assemblies upon binding with CB[7] was carried out with AuNPs having different surface functional groups (Fig. 2 (b)). AuNP-ADA (1 μM) and AuNP-TMC6 (1 μM) behaved similar to AuNP-TBen and induced the large assemblies upon binding with CB[7] at the ratio of 1:10 (AuNPs:CB[7]).

In contrast, AuNP-TMOH and AuNP-TMNH2 did not show any aggregate formation although the NP-CB[7] complexes were formed as indicated in ¹H NMR and NOESY NMR (Supporting Fig. 5-8). This indicates that the surface end group of the AuNPs plays an important role in inducing the assembly formation.

The amphiphilic nanoparticle, AuNP-TBen (also AuNP-ADA and AuNP-TMC6) is soluble in both aqueous and organic solvents (e.g. dichloromethane). In the aqueous solution, the hydrophobic benzyl units on the particles are hidden from the external environment, making the surface of the particles more hydrophilic and soluble in the aqueous media. NOESY NMR showed the interaction of benzyl peaks with tetraethylene glycol and 11-undecane peaks (Supporting Fig. 9) as an indication of bending over of benzyl head group. Addition of CB[7] resulted in a binding competition of pulling AuNP-TBen from its hydrophobic shell to be encapsulated by CB[7] host molecules. Upon binding with CB[7], the benzyl units on the particle became stretched out along the particle, rendering the surface of the particle less hydrophilic. This process decreases particle solubility and induces the formation of large assemblies/aggregates (Fig. 1 (b)). AuNP-TMOH and AuNP-TMNH2 can bind with CB[7] but the hydroxyl and amine end groups presumably keep the surface of particles hydrophilic enough even after binding with CB[7] and therefore no assembled structures were observed.

It indicates that inducing assemblies is dependent on not only CB[7] binding but also end group surface functionality of AuNPs.

When the particle assemblies of AuNP-TBen-CB[7] were treated with excess of 1-adamantyl amine (ADA), a competitive guest molecule for CB[7] binding, CB[7] dethreaded from the NP surface through creation of more favorable 1:1 ADA-CB[7] complexes ($K_a = 1.7 \times 10^{12}$).^{21c} Addition of ADA triggered disassembly of the particles, (Supporting Fig. 10), indicating that host-guest interaction can be used to control the solubility (hydrophobicity) of AuNPs by using the precise 'lock and key' modulation over their molecular-level interactions.

Cellular uptake behavior of the AuNPs were investigated by TEM analysis of the cell. After 3 h incubation of the cationic AuNP-TBen (200 nM), TEM images showed that the AuNPs were trapped in the endosomal vesicles in cytoplasm as shown in Fig. 3 (a). This observation is consistent with an endocytotic behavior of other cationic nanoparticles previously reported in literature.^{30,31} To study the exocytotic behaviors of the nanoparticle, the cells were washed off after 3 h incubation with the AuNP-TBen and incubated with fresh media or CB[7] (0.2 mM) containing media for an additional 24 h. When the cells were treated by fresh media, the number of the particle-entrapped in vesicles was significantly decreased (Fig. 3 (b)). Only a few particles remained within the vesicles or dispersed in various organelles, indicating a major portion of the AuNP-TBen are removed from the cells through exocytosis. In contrast, when the cells were treated by the CB[7] containing media, complexation between the CB[7] and AuNPs occurred in endosomes and in turn the AuNPs remained trapped in the endosomes (Fig. 3 (c)).¹⁹ These results indicate that treatment of CB[7] caused the intracellular assembly formation of the AuNP-TBen-CB[7] as the CB[7] can cross the cell membrane³² and the large bulky assemblies remained sequestered in endocytic vesicles without exocytosis. It is important to note that CB[7] can be internalized by cells as free CB[7] and/or nanoparticle-bound CB[7] have been detected inside cells using mass spectrometry.¹⁷

The exocytosis of the nanoparticles was further quantified by using inductively coupled plasma mass spectrometry (ICP-MS). After 3 h incubation of AuNP-TBen (200 nM), the cells were completely washed off and replaced by fresh cell culture media or CB[7] (0.2 mM) containing media. The cells were then further incubated for different time intervals (0 h, 3 h, 12 h, and 24 h). The amount of the AuNPs retained by the cells was determined by using ICP-MS. Retention of the AuNP-TBen inside cells treated by free cell culture media decreased to 34 % at 24 h while no significant change was observed for cells treated with CB[7] containing media (Fig. 3 (d)). Along with the observed TEM results, ICP-MS data shows that the treatment of the CB[7] on the cells effectively inhibited the exocytosis of the AuNP-TBen.

The effect of the AuNP end group on the exocytosis was further investigated and the retention of other AuNPs with different functional head groups in the cells was measured by using ICP-MS. AuNP-TTMA and AuNP-TMOH (Fig. 4 (a) and (b)) exhibited no significant difference of exocytotic behavior for both free media and media containing CB[7], showing no effect of CB[7] on exocytosis of these AuNPs.

Regardless of CB[7] treatment, retention of the AuNP-TTMA and AuNP-TMOH decreased to ~ 62 % and ~ 70 % at 24 h, respectively. Compared to AuNP-TBen, AuNP-TTMA and AuNP-TMOH showed higher retention inside cells. This different behavior could be originated from the surface functionality of AuNPs as aromatic head group structure of AuNP-TBen resulted in faster exocytosis rate.²⁵ On the other hand, exocytosis of AuNPs including AuNP-ADA and AuNP-TMC6 was blocked when the cells were treated by the media containing CB[7] similar to the AuNP-TBen (Fig. 4 (c) and (d)). Amount of the retained AuNP-ADA and AuNP-TMC6 in the cells reduced to ~ 75 % and ~ 70 % at 24 h for the media treatment. Both AuNP-ADA and AuNP-TMC6 induced assemblies of the particle upon binding with CB[7]. This result indicates that CB[7] itself does not affect cellular uptake of the particles and exocytosis of the particles was regulated due to the increased size of the assemblies.

Cellular proliferative activity was measured by the Alamar blue assay to evaluate possible toxicity that can arise from retained nanoparticles in the cells. As shown in Fig. 5, all the nanoparticles exhibited no decrease in cell viability for the treatment of both free media and media containing CB[7]. This result indicates that the induced assemblies of the particles sequestered in endocytic vesicles do not affect cell viability.

Conclusions

In conclusion, we have demonstrated a strategy for regulating exocytosis of the internalized nanoparticles. Using a supramolecular host-guest system on the AuNPs induced the assemblies of the particles in the living cells, preventing their exocytosis without any observed cytotoxicity. This approach provides a potential strategy for prolonged retention of drug carriers within endosomes, enabling sustained therapeutic effect of the carriers. We are currently exploring this strategy with AuNPs featuring prodrugs tethered with labile linkages that can be degraded by external stimuli. Additionally, this approach also will be applied to other nanomaterials with potential utility of their prolonged transplantation in a wide variety of cells for *in vivo* cellular tracking³³ and tumor- targeted delivery of therapeutic systems.³⁴

Experimental section General

Synthesis of ligands and AuNPs and their characterization can be found in Supporting Information. All the chemicals were purchased from Sigma-Aldrich or Fisher Scientific unless otherwise specified. The chemicals were used as received. AuNPs used in this work have been reported previously.³⁵ ¹H NMR spectra were recorded at 400 MHz on a Bruker AVANCE 400 machine. A Hewlett-Packard 8452A UV-Vis spectrophotometer was used to record UV-Vis spectra. Dynamic light scattering (DLS) was measured by Zetasizer Nano ZS. The fluorescence from the Alamar blue assay was measured in a SpectraMax M5 microplate spectrophotometer.

ICP-MS sample preparation and measurements

ICP-MS measurements were performed on a Perkin Elmer Elan 6100. Operating conditions of the ICP-MS are listed below: RF power: 1200 W; plasma Ar flow rate: 15 L/min; nebulizer Ar flow rate: 0.96 L/min; isotopes monitored: ¹⁹⁷Au; dwell time: 50 ms; nebulizer:

cross flow; spray chamber: Scott. AuNPs (200 nM, 0.5 ml) were incubated with pre-seeded MCF-7 cell line in 24 well plates (20,000 cells/well). After 3 h incubation, cells were washed three times with PBS buffer and then 0.5 mL of media or media of CB[7] (0.2 mM) was added to the cells. The wells of the plates then connected to a peristaltic pump which provides a continuous flow of the media or media of CB[7] to remove exocytosed nanoparticles. The cells were then incubated for different additional times (0 h, 3 h, 12 h, and 24 h). Cells were washed three times with PBS buffer and then a lysis buffer (300 μ l) was added to the cells. The resulting cell lysate was digested overnight using 3 mL of HNO₃ and 1 mL of H₂O₂. On the next day, 3 mL of aqua regia was added and then the sample was allowed to react for another 2-3 h. The sample solution was then diluted to 100 mL with de-ionized water and aqua regia. The final AuNP sample solution contained 5% aqua regia. The AuNP sample solution was measured by ICP-MS under the operating conditions described above. Cellular uptake experiments with each gold nanoparticle were repeated 3 times, and each replicate was measured 5 times by ICP-MS. A series of gold standard solutions (20, 10, 5, 2, 1, 0.5, 0.2, 0 ppb) were prepared before each experiment. Each gold standard solution contained 5% aqua regia. The resulting calibration line was used to determine the gold amount taken up in the cells in each sample.

Cellular TEM measurements

For a preparation of cellular TEM samples, MCF-7 cells (100,000 cells per well in a 24 well plate) were seeded and incubated on 15 mm diameter Thermanox® coverslips (Nalge Nunc International, NY) in 1 mL of serum containing media for 24 h prior to the experiment. The media was replaced by 0.5 mL of 200 nM AuNPTBen in serum containing media and incubated for 3 h. The cells were completely washed with PBS buffer three times and then 0.5 mL of media or media of CB[7] (0.2 mM) was added to the cells. After 24 h incubation, the cells were then fixed in 2 % glutaraldehyde with 3.75 % sucrose in 0.1 M sodium phosphate buffer (pH 7.0) for 30 min and then washed with 0.1 M PBS containing 3.75% sucrose three times over 30 min. The cells were postfixed in 1 % osmium tetroxide with 5 % sucrose in 0.05 M sodium phosphate buffer solution (pH 7.0) for 1 hr and then rinsed with distilled water three times. They were dehydrated in a graded series of acetone (10 % per step) and embedded in epoxy resin. The resin was polymerized at 70 °C for 12 h. Ultrathin sections (50 nm) obtained with a Reichert Ultracut E Ultramicrotome and imaged under a JEOL 100S electron microscopy.

Cell culture and cytotoxicity measurements

MCF-7 cells were grown in a cell culture flask using low glucose Dulbecco's Modified Eagle Medium supplemented with 10% fetal bovine serum (FBS) at 37°C in a humidified atmosphere of 5% CO₂. For cytotoxicity testing, MCF-7 cells were seeded at 20,000 cells in 0.2 mL per well in a 96-well plate 24 h prior to the experiment. During the experiment, old media was replaced by 0.2 mL of AuNPs (200 nM) in serum containing media and the cells were incubated for 3 h at 37°C in a humidified atmosphere of 5 % CO₂. The cells were then completely washed with PBS buffer three times and media or media of CB[7] (0.2 mM) was added to the cell. After 24 h of incubation, the cells were then completely washed off and 10% Alamar Blue in serum containing media was added to each well and further incubated

at 37 °C for 4 h. The cell viability was then determined by measuring the fluorescence intensity at 570 nm using a SpectraMax M5 microplate spectrophotometer.

Supplementary Material

Refer to Web version on PubMed Central for supplementary material.

Acknowledgements

This work was supported by the NIH (NIH R01 EB014277-01).

References

1. a Allen TM, Cullis PR. *Science*. 2004; 303:1818. [PubMed: 15031496] b Nicolas J, Mura S, Brambilla D, Mackiewicz N, Couvreur P. *Chem. Soc. Rev.* 2013; 42:1147. [PubMed: 23238558] c Kudgus RA, Walden CA, McGovern RM, Reid JM, Robertson JD, Mukherjee P. *Sci. Rep.* 2014 doi:10.1038/srep05669.
2. Tonga GY, Moyano DF, Kim CS, Rotello VM. *Curr. Opin. Colloid Interface Sci.* 2014; 19:49. [PubMed: 24955019]
3. a Li W-P, Liao P-Y, Su C-H, Yeh C-S. *J. Am. Chem. Soc.* 2014; 136:10062. [PubMed: 24953310] b Peer D, Karp JM, Hong S, Farokhzad OC, Margalit R, Langer R. *Nat. Nanotechnol.* 2007; 2:751. [PubMed: 18654426] c Torchilin VP. *J. Controlled Release.* 2001; 73:137.
4. a Zhang X-Q, Xu X, Lam R, Giljohann D, Ho D, Mirkin CA. *ACS Nano.* 2011; 5:6962. [PubMed: 21812457] b Bansal A, Zhang Y. *Acc. Chem. Res.* 2014; 47:3052. [PubMed: 25137555] c Pietrzak-Nguyen A, Fichter M, Dedters M, Pretsch L, Gregory SH, Meyer C, Doganci A, Diken M, Landfester K, Baier G, Gehring S. *Biomacromolecules.* 2014; 15:2378. [PubMed: 24901387]
5. a Cohen K, Emmanuel R, Kisin-Finifer E, Shabat D, Peer Dan. *ACS Nano.* 2014; 8:2195. b Doane TL, Burda Clemens. *Chem. Soc. Rev.* 2012; 41:2885. [PubMed: 22286540]
6. a Duncan R. *Nat. Rev. Drug. Discov.* 2003; 2:347. [PubMed: 12750738] b Agasti SS, Chompoosor A, You CC, Ghosh P, Kim CK, Rotello VM. *J. Am. Chem. Soc.* 2009; 131:5728. [PubMed: 19351115] c Hong R, Han G, Fernandez JM, Kim BJ, Forbes NS, Rotello VM. *J. Am. Chem. Soc.* 2006; 128:1078. [PubMed: 16433515] d Timko BP, Dvir T, Kohane DS. *Adv. Mater.* 2010; 22:4925. [PubMed: 20818618] e Tonga GY, Saha K, Rotello VM. *Adv. Mater.* 2014; 26:359. [PubMed: 24105763]
7. a Perrault SD, Walkey C, Jennings T, Fischer HC, Chan WCW. *Nano Lett.* 2009; 9:1909. [PubMed: 19344179] b Matsumura Y, Maeda H. *Cancer Res.* 1986; 46:6387. [PubMed: 2946403]
8. a Choia CHJ, Alabia CA, Webster P, Davisa ME. *Proc. Natl. Acad. Sci. USA.* 2010; 107:1235. [PubMed: 20080552] b Sykes EA, Chen J, Zheng G, Chan WCW. *ACS Nano.* 2014; 8:5696. [PubMed: 24821383]
9. a Chithrani BD, Chan WCW. *Nano. Lett.* 2007; 7:1542. [PubMed: 17465586] b Klostranec JM, Chan WCW. *Adv. Mater.* 2006; 18:1953.
10. a Panyam J, Zhou WZ, Prabha S, Sahoo SK, Labhasetwar V. *Faseb. J.* 2002; 16:1217. [PubMed: 12153989] b Panyam J, Labhasetwar V. *Mol. Pharmaceut.* 2004; 1:77.
11. Pickett JA, Edwardson JM. *Traffic.* 2006; 7:109. [PubMed: 16420520]
12. a Slowing II, Vivero-Escoto JL, Zhao Y, Kandel K, Peeraphatdit C, Trewyn BG, Lin VSY. *Small.* 2011; 7:1526. [PubMed: 21520497] b Chavanpatil MD, Handa H, Mao G, Panyam J, Biomed J. *Nanotechnol.* 2007; 3:291.
13. Panyam J, Labhasetwar V. *Pharmaceut. Res.* 2003; 20:212.
14. a Vasir JK, abhasetwar VL. *Biomaterials.* 2008; 29:4244. [PubMed: 18692238] b Sahoo SK, Labhasetwar V. *Mol. Pharmaceut.* 2005; 2:373.
15. a Lehn, JM. *Supramolecular Chemistry: Concepts and Perspectives.* VCH; New York: 1995. b Petkau-Milroy K, Brunsveld L. *Org. Biomol. Chem.* 2013; 11:219. [PubMed: 23160566]

16. a Angelos S, Yang YW, Patel K, Stoddart JF, Zink JI. *Angew. Chem. Int. Edit.* 2008; 47:2222. b Angelos S, Khashab NM, Yang YW, Trabolsi A, Khatib HA, Stoddart JF, Zink JI. *J. Am. Chem. Soc.* 2009; 131:12912. [PubMed: 19705840] c Coti KK, Belowich ME, Liong M, Ambrogio MW, Lau YA, Khatib HA, Zink JI, Khashab NM, Stoddart JF. *Nanoscale.* 2009; 1:16. [PubMed: 20644858] d Klajn R, Olson MA, Wesson PJ, Fang L, Coskun A, Trabolsi A, Soh S, Stoddart JF, Grzybowski BA. *Nat. Chem.* 2009; 1:733. [PubMed: 21124361]
17. Yan B, Tonga GY, Hou S, Fedick PW, Yeh Y-C, Alfonso FS, Mizuhara T, Vachet RW, Rotello VM. *Anal. Chem.* 2014:86.
18. a Lim YB, Kim T, Lee JW, Kim SM, Kim HJ, Kim K, Park JS. *Bioconjugate Chem.* 2002; 13:1181. b Kim SK, Park KM, Singha K, Kim J, Ahn Y, Kim K, Kim WJ. *Chem. Commun.* 2010; 46:692. c Ghosh S, Isaacs L. *J. Am. Chem. Soc.* 2010; 132:4445. [PubMed: 20210325]
19. Kim C, Agasti SS, Zhu ZJ, Isaacs L, Rotello VM. *Nat. Chem.* 2010; 2:962. [PubMed: 20966953]
20. Kim J, Ahn Y, Park KM, Kim Y, Ko YH, Oh DH, Kim K. *Angew. Chem. Int. Edit.* 2007; 46:7393.
21. a Kim K, Selvapalam N, Ko YH, Park KM, Kim D, Kim J. *Chem. Soc. Rev.* 2007; 36:267. [PubMed: 17264929] b Gamal-Eldin MA, Macartney DH. *Org. Biomol. Chem.* 2013; 11:1234. [PubMed: 23314170] c Lagona J, Mukhopadhyay P, Chakrabarti S, Isaacs L. *Angew. Chem. Int. Edit.* 2005; 44:4844.
22. a Hettiarachchi G, Nguyen D, Wu J, Lucas D, Ma D, Isaacs L, Briken V. *Plos One.* 2010; 5:e10514. [PubMed: 20463906] b Uzunova VD, Cullinane C, Brix K, Nau WM, Day AI. *Org. Biomol. Chem.* 2010; 8:2037. [PubMed: 20401379]
23. a Kim CK, Ghosh P, Rotello VM. *Nanoscale.* 2009; 1:61. [PubMed: 20644861] b Ghosh P, Han G, De M, Kim CK, Rotello VM. *Adv. Drug Deliver. Rev.* 2008; 60:1307.
24. a Saha K, Kim ST, Yan B, Miranda OR, Alfonso FS, Shlosman D, Rotello VM. *Small.* 2013; 9:300. [PubMed: 22972519] b Verma A, Uzun O, Hu Y, Hu Y, Han H-S, Watson N, Chen S, Irvine DJ, Stellacci F. *Nature Mater.* 2008; 7:588. [PubMed: 18500347]
25. Kim CS, Le NDB, Xing Y, Yan B, Tonga GY, Kim C, Vachet RW, Rotello VM. *Adv. Healthc. Mater.* 2014; 3:1200. [PubMed: 24665047]
26. Nam J, Won N, Jin H, Chung H, Kim S. *J. Am. Chem. Soc.* 2009; 131:13639. [PubMed: 19772360]
27. Templeton AC, Wuelfing MP, Murray RW. *Acc. Chem. Res.* 2000; 33:27. [PubMed: 10639073]
28. Yuan LN, Wang RB, Macartney DH. *Tetrahedron: Asymmetry.* 2007; 18:483.
29. Wheate NJ. *J. Inorg. Biochem.* 2008; 102:2060. [PubMed: 18653238]
30. Zhu ZJ, Ghosh PS, Miranda OR, Vachet RW, Rotello VM. *J. Am. Chem. Soc.* 2008; 130:14139. [PubMed: 18826222]
31. Kim CK, Ghosh P, Pagliuca C, Zhu ZJ, Menichetti S, Rotello VM. *J. Am. Chem. Soc.* 2009; 131:1360. [PubMed: 19133720]
32. Montes-Navajas P, Gonzalez-Bejar M, Scaiano JC, Garcia H. *Photoch. Photobio. Sci.* 2009; 8:1743.
33. Bulte JWM, Kraitchman DL. *Nmr. Biomed.* 2004; 17:484. [PubMed: 15526347]
34. Roger M, Clavreul A, Venier-Julienne MC, Passirani C, Montero-Menei C, Menei P. *Biomaterials.* 2011; 32:2106. [PubMed: 21183214]
35. Tang R, Moyano DF, Subramani C, Yan B, Jeoung E, Tonga GY, Duncan B, Yeh Y-C, Jiang Z, Kim C, Rotello VM. *Adv. Mater.* 2014; 26:3310. [PubMed: 24677290]

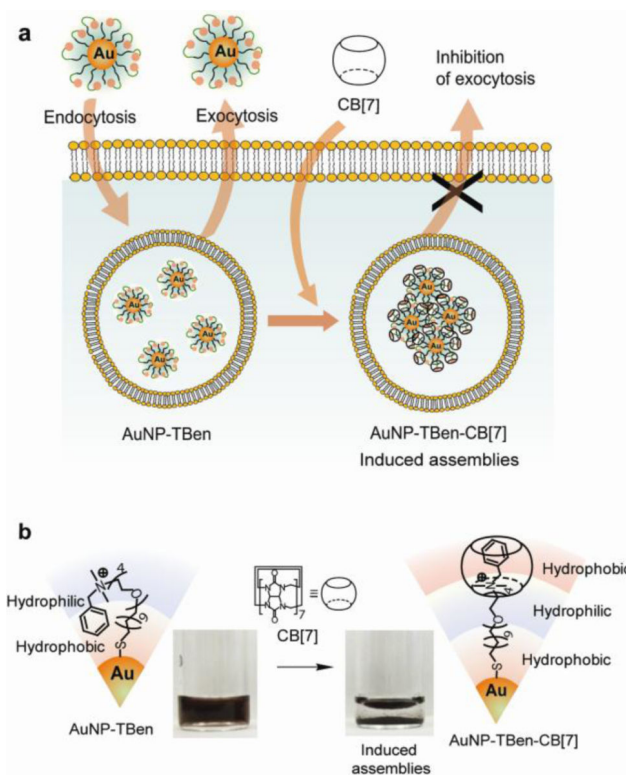


Fig. 1. Controlling exocytosis of AuNPs by using intracellular host-guest complexation
(a) Inhibition of AuNP-TBen exocytosis by the threading of CB[7] onto the nanoparticle surface. (b) Formation of the AuNP-TBen-CB[7] assemblies.

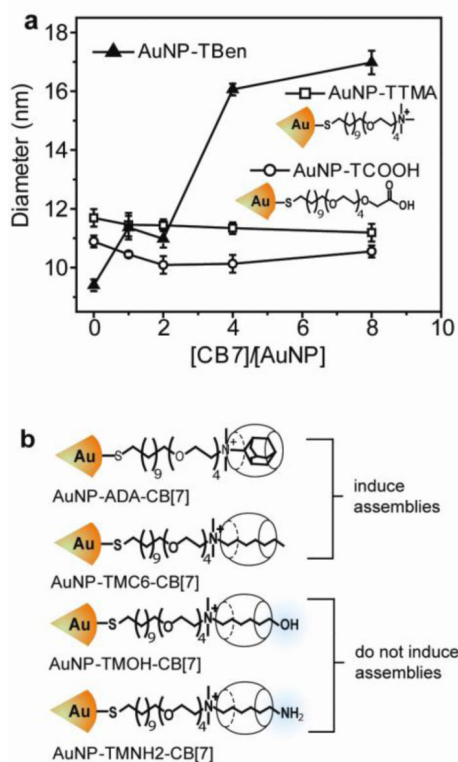


Fig 2. Inducing nanoparticle assemblies upon binding with CB[7] and the effect of surface functional group on the assembly formation
 (a) Size changes of nanoparticle assemblies at different NP:CB[7] ratios. (b) AuNP-ADA and AuNP-TMC6 induce the larger assemblies upon binding with CB[7], but no assembly formation was observed for AuNP-TMOH and AuNP-TMNH2 with polar end groups.

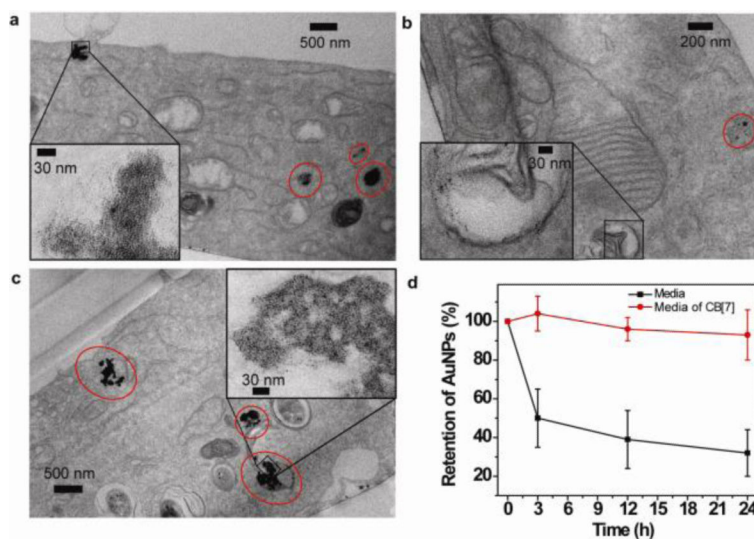


Fig. 3. Cellular uptake and intracellular behavior of the AuNPs

(a) TEM images of MCF-7 cells incubated with AuNP-TBen. The cationic AuNP-TBen is trapped in organelles (red circle). TEM images MCF-7 cells incubated with AuNP-TBen and then washed and further incubated with (b) only cell culture media or (c) culture media with CB[7] for 24 h. (d) Quantification of the amount of gold retained in cells at different time after incubation with free media or media containing CB[7]. Cellular uptake experiments with each gold nanoparticle were repeated 3 times, and each replicate was measured 5 times by ICP-MS. Error bars represent the standard deviations of these measurements.

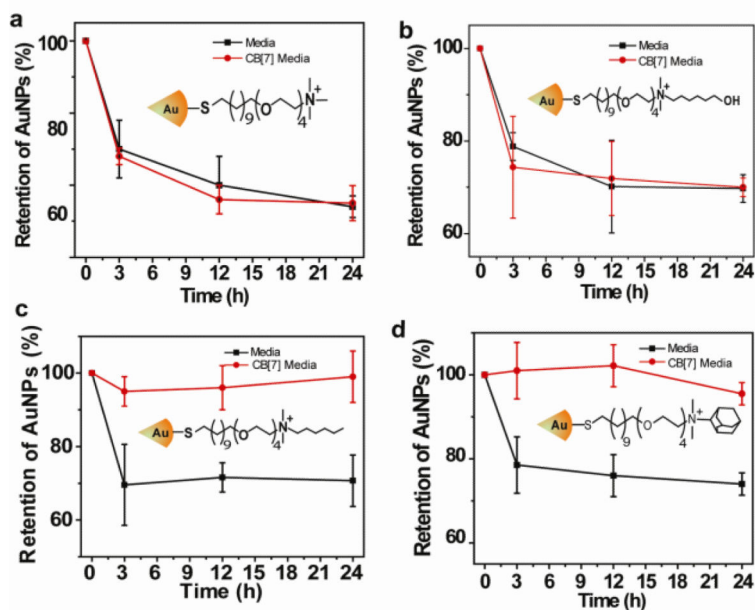


Fig. 4. Effect of surface functional groups on exocytotic behavior of AuNPs
ICP-MS measurements of (a) AuNP-TTMA, (b) AuNP-TMOH, (c) AuNP-TMC6, and (d) AuNP-ADA. Quantification of exocytosis of the AuNPs was determined by analyzing ICP-MS on MCF-7 cell with same experimental condition carried out for the AuNP-TBen. Error bars represent the standard deviations of these measurements.

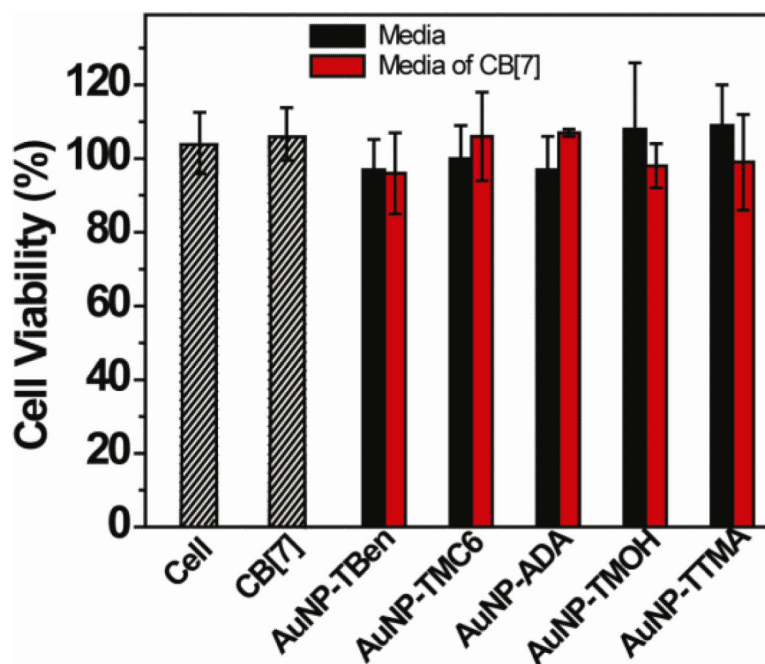


Fig. 5. Cytotoxicity of AuNPs

After 3h incubation of AuNPs (200 nM), MCF-7 cells were washed off and further incubated with media and media of CB[7] (0.2 mM) at 37 °C for 24 h. As a control, cell viability of CB[7] (0.2 mM) was measured after 24 h incubation.